LA-UR-19-20453
Approved for public release; distribution is unlimited.

Title: ZEUS Activation Foils Report for Experiments 1-5

Author(s): Moss, Calvin Elroy
Bounds, John Alan
Jaegers, Peter James

Intended for: Report

Issued: 2019-01-22

# ZEUS Activation Foils Report for Experiments 1-5

**Calvin Moss, John Bounds, and Peter Jaegers**

## Introduction

The ZEUS experiments were conducted using the COMET vertical assembly machine at the Los Alamos Critical Experiments Facility (LACEF) at the Los Alamos National Laboratory (LANL). The experiments were designed to check the adequacy of cross sections in the intermediate-energy range. For the first four experiments, 12 kg highly enriched uranium (HEU) layers were sandwiched between different numbers of graphite plates in a vertical stack. In the first four experiments, a unit cell consisted of n graphite plates, an HEU layer, and then another n graphite plates. The unit cells were stacked until criticality was obtained. Experiments 1, 2, 3, and 4 contained decreasing amounts of graphite, where the unit cells value n was 4, 3, 2 and 1 respectively. In experiment 5 the HEU plates were in direct contact with each other to evaluate cross sections in the fast-energy range. A detailed description of experiments 1-4 is provided in reference [1], and of experiment 5, in reference [2].

In order to investigate the cross sections in more detail, some ZEUS runs were made with activation foils inside the assemblies. Ratios of the activations of various foils are a standard method of measuring the gross neutron spectrum shape. A more detailed spectrum can be determined by simultaneously unfolding the response of several foils. This report describes the unfolding of the ZEUS activation foils data. The focus in this analysis is on the fast-energy range, especially at > 5 MeV.

## Unfolding Codes

Activation foils can be used to measured neutron spectra when other techniques, such as time of flight or scintillation detectors, are not possible. The foil is exposed to the neutron flux for a period of time and then removed so that the induced radioactivity may be counted, typically using gamma and beta counting methods. The different materials in the foils respond differently because cross sections for the reactions on each material are different. These differences can be used to determine the neutron spectrum with unfolding analysis. Basically, a trial spectrum is varied, subject to some constraints, to give the best simultaneous fit to the induced activities in all of the foils. In many cases the code will calculate an acceptable spectrum when the trial spectrum is only a rough approximation of the expected finally fitted spectrum. However, the final spectrum may be more accurate when the trial spectrum is close to the final spectrum.

Several analysis methods with corresponding computer programs have been developed to do the unfolding. One of the early uses of activation foils was the measurement at Los Alamos of the spectra from the fission of $^{235}$U, $^{233}$U, and $^{239}$Pu [3]. In 1967, SAND-II, developed at the Kirkland Air Force Weapons Laboratory, was published [4]. In 1994, Sandia National Laboratory published an improved version of the SAND-II code and a user's manual [5]. The neutron spectrum at the Missouri University of Science and Technology Research Reactor was determined with the SAND II code [6]. The neutron spectrum from the Target-Moderator-Reflector-1 at the Indiana University was also characterized with the SAND-II code [7]. These early codes lacked adequate constraints on the fits, especially when the response functions contained resonances. More recently, several different codes and applications have been reported. GRAVEL is a slightly modified version of SAND-II and has been used for some measurements [8]. Dehimi *et al.* proposed unfolding with Fisher Regularisation [9]. Many of the codes, including SAND II, require a trial spectrum as *a-prior* input. The GAMCD (Genetic Algorithm and Monte Carlo Deconvolution) was developed by a group in India and does not require *a-prior* input. GAMCD was used to measure the neutron spectrum from the p+Be reaction at 20 MeV [10]. The MINUIT code in the CERN Cernlib, with smoothness and shape constraints, was used by researchers from Algeria to unfolded reactor data [11]. Tripathy *et al.*compare several different unfolding codes [12]. For the present report, we chose to use the Few Channel Maximum Entropy (MAXED) code, which was part of the U_M_G (Unfolding and Maxed and Gravel) version 3.3 code prepared by Reginatto *et al.* at the Physikalisch-Technische Bundesanstalt (PTB) in Germany because it was the only one readily available, except for the older code SAND II and its slight revised version GRAVEL [13]. The code and the manual were obtained from the Radiation Safety Information Computational Center (RSICC) at the Oak Ridge National Laboratory.

## MAXED Unfolding Code

The MAXED code received from RSICC was a FORTRAN program. It contains 34 subroutines, and the most important one is the SA subroutine. SA implements the continuous simulated annealing global optimization algorithm by trying to find the global optimum of an N dimensional function. Initially, the code would not compile with the GFORTRAN compiler running on a PC. The code contained commands from FORTRAN 77, FORTRAN 90, and probably other versions. It also contained commands that were required for some specific computers. After these were modified or removed, the program did compile. Next, simple test data, which were supplied with the code for Bonner spheres, were attempted, and the results were not correct. Print debugging statements were inserted in the program to locate the problems and then make modifications. Now, the program can process a set of foils data in approximately two minutes or less.

The input MAXED files are the following.

1. Control file, which contains names of other files and fitting parameters
2. Measured data
3. Response functions
4. Output file name
5. Default spectrum

The Appendix provides some partial examples of these files.

### Response Functions

The response function for a reaction is equal to the cross section for the reaction multiplied by the number of target isotope nuclei in the foil. For the present analysis, 640 energy bins were chosen in order to provide sufficient detail of structure in the spectrum. This choice is a standard that has been used in other published reports [5]. The MCNP code was used to bin the ENDF VII cross sections into 640 bins. MCNP was also used to bin the cross sections when the foils were covered with cadmium to eliminate low-energy reactions. Figure 1 shows plots of the effective cross sections. Without a cadmium cover, the plotted cross sections are just the binned ENDF VII cross sections. With a cadmium cover, the cross sections have been corrected by the attenuation of the neutrons by the cadmium to provide effective cross sections. The cross sections for the (n,g) reactions at < 100 keV are very large, but the focus in this report is on the fast-energy range, especially at > 5 MeV.

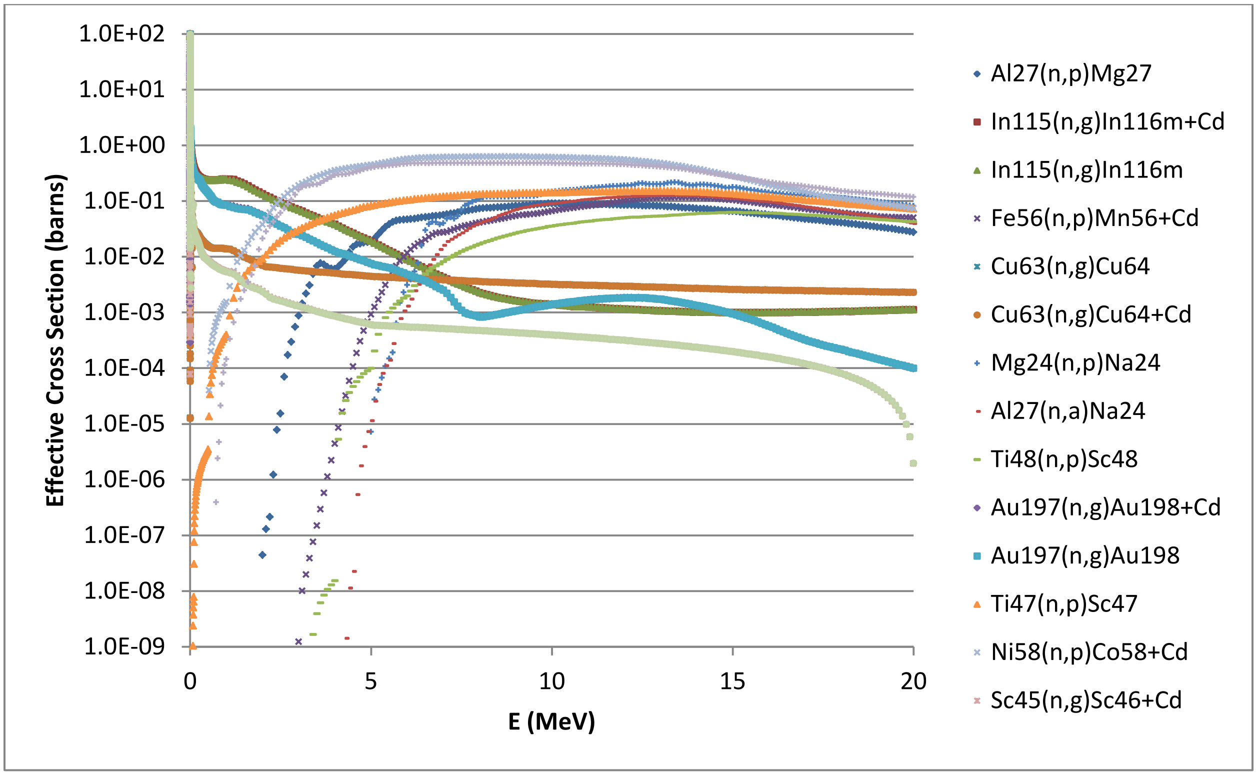


Figure 1. Comparison of the effective cross sections calculated into 640 bins with MCNP.

## Default Spectra

The trial spectra were also calculated with MCNP using the detailed MCNP models in references [1,2]. The $^{235}U$ cross sections from ENDF/B-VI were used for the trial spectra because these cross sections were the ones being tested at the time of the ZEUS measurements. The spectra were calculated in the sample holes in the sample plate without samples in the holes. The default spectra are shown in Figures 3-7 below in the Analysis of the ZEUS Foils section.

## Analysis of the ZEUS Foils

Gamma spectra from all of the foils were measured with a germanium detector after they were irradiated. The counts in the largest gamma-ray peaks were calculated with the Peak Easy code [14]. The ratio of the number of activated nuclei to the total number of target nuclei for each reaction was calculated using EXCEL spreadsheets. Corrections were made for the detector efficiency, branching ratio, mass of the foil, isotopic abundance, length of time of the irradiation, time from end of irradiation until the start of the gamma measurement, and the length of time of the measurement. When several gamma-ray branches had good statistics, a weighted average was calculated.

ZEUS Experiment 1

For this experiment the core loading contained 10 units. Each unit contained one inner HEU disk and one outer HEU ring sandwiched in the middle of eight graphite plates. Reference [1] provides details. The foils were located in recessed holes in an aluminum plate, shown in Figure 2. This plate was located between units 4 and 5. Table 1 lists the data from the gamma-ray measurements of the activated foils. The ratio is the number of activated nuclei divided by the number of target nuclei. Corrections were made for the isotopic abundance, detector efficiency, gamma-ray branching ratio, decay since the end of the irradiation, and decay during the gamma-ray measurement decay.

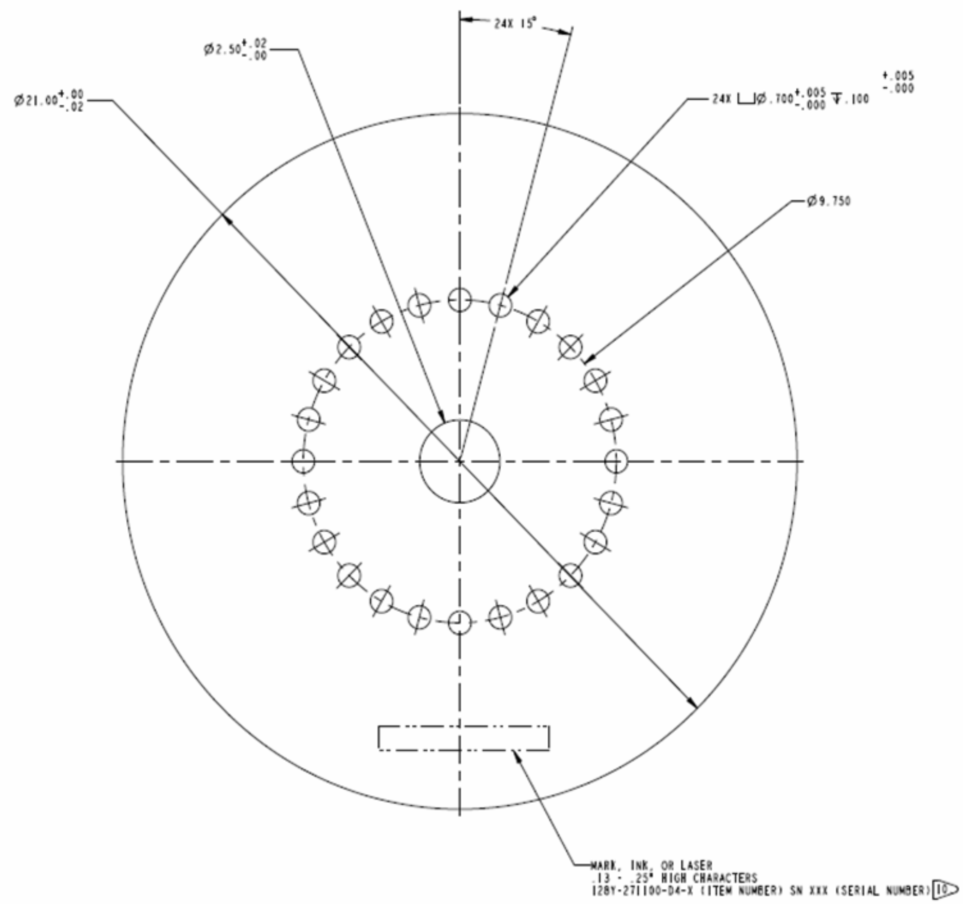


Figure 2. Aluminum sample plate 0.125 inch thick with 24 recessed holes for the foils [15].

Table 1. Experiment 1 Foil Data

| Reaction | Cd Cover? | Isotopic Abundance (%) | Half-life | Ratio |
|---|---|---|---|---|
| In115(n,g)In116m | yes | 95.70 | 54 m | 5.048(25)E-11 |
| In115(n,g)In116m | no | 95.70 | 54 m | 4.955(26)E-11 |
| Fe56(n,p)Mn56 | yes | 91.72 | 2.57 h | 4.94(36)E-15 |
| Cu63(n,g)Cu64 | no | 69.17 | 12.8 h | 4.636(17)E-12 |
| Cu63(n,g)Cu64 | yes | 69.17 | 12.8 h | 4.480(16)E-12 |
| Mg24(n,p)Na24 | no | 78.99 | 15.06 h | 5.4(1.7)E-15 |
| Al27(n,a)Na24 | no | 100.00 | 15.06 h | 2.96(22)E-15 |
| Ti48(n,p)Sc48 | no | 73.80 | 44 h | 1.80(55)E-15 |
| Au197(n,g)Au198 | yes | 100.0 | 2.69 d | 9.785(25)E-11 |
| Au197(n,g)Au198 | no | 100.0 | 2.69 d | 9.559(25)E-11 |
| Ti47(n,p)Sc47 | no | 7.30 | 3.43 d | 1.139(72)E-13 |
| Ni58(n,p)Co58 | yes | 68.27 | 72 d | 6.606(86)E-13 |
| Sc45(n,g)Sc46 | no | 100.0 | 85 d | 2.849(12)E-12 |
| Sc45(n,g)Sc46 | yes | 100.0 | 85 d | 2.660(17)E-12 |
| Fe54(n,p)Mn54 | yes | 5.80 | 310 d | 2.0(1.7)E-13 |

The GAMED code was run with this foil data. A 640-bin trial spectrum was calculated with an F4 tally in the holes in the sample plate without foils present. The details of the MCNP model, without the sample plate, are available in reference [1].

Figure 3 shows a comparison of the fitted spectrum with the trial spectrum. The statistical uncertainty increases at high energies in both the fit spectrum and the trial spectrum. Note that error bars for each energy bin are not shown because the MAXED code does not calculate them. The fit closely matches the trial spectrum below 6500 keV, but above 6500 keV, the fitted spectrum is higher. This may indicate that the $^{235}U$ cross sections, on which the trial spectrum is based, are too low at high energies.

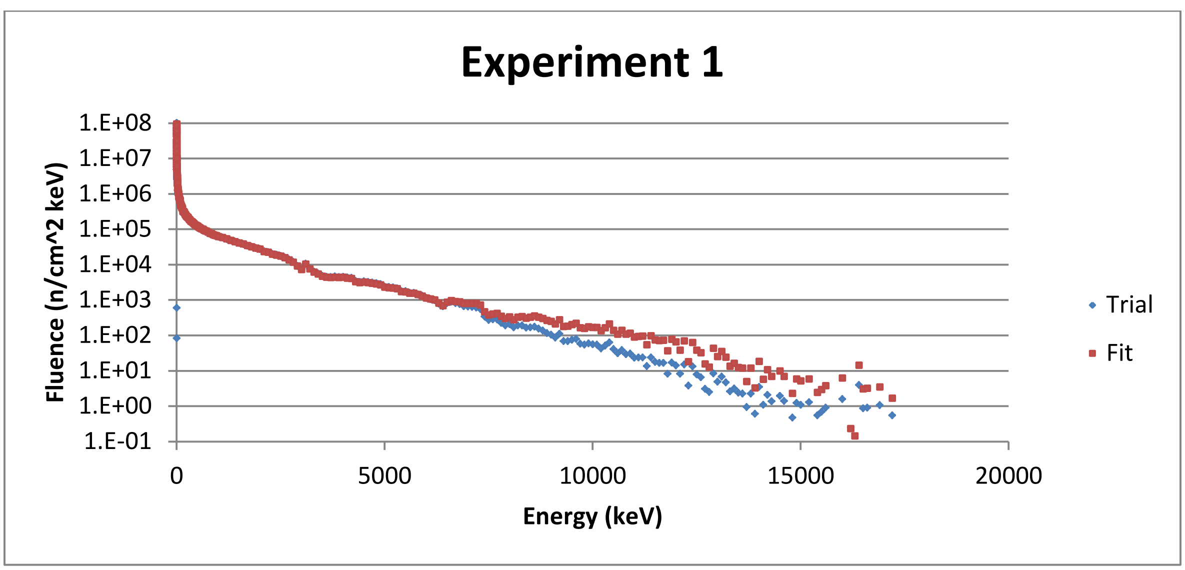


Figure 3. Comparison of the MCNP trial spectrum and the spectrum determined by unfolding the activation foils data for experiment 1, which had 8 graphite plates per unit.

ZEUS Experiment 2

This experiment was similar to experiment 1, but the core loading contained 9 units. Each unit contained one inner HEU disk and one outer HEU ring sandwiched in the middle of six graphite plates. The sample plate was located between units 2 and 3. Table 2 lists the data from the gamma-ray measurements of the activated foils.

Table 2. Experiment 2 Foil Data

| Reaction | Cd Cover? | Isotopic Abundance (%) | Half-life | Ratio |
|---|---|---|---|---|
| Al27(n,p)Mg27 | no | 100.0 | 9.45 min | 1.794(42)E-14 |
| In115(n,g)In116m | yes | 95.70 | 54 m | 9.063(22)E-11 |
| In115(n,g)In116m | no | 95.70 | 54 m | 9.312(25)E-11 |
| Fe56(n,p)Mn56 | yes | 91.72 | 2.57 h | 1.174(44)E-14 |
| Cu63(n,g)Cu64 | no | 69.17 | 12.8 h | 1.142(3)E-11 |
| Cu63(n,g)Cu64 | yes | 69.17 | 12.8 h | 1.156(3)E-11 |
| Mg24(n,p)Na24 | no | 78.99 | 15.06 h | 1.83(18)E-14 |
| Al27(n,a)Na24 | no | 100.00 | 15.06 h | 8.01(28)E-15 |
| Ti48(n,p)Sc48 | no | 73.80 | 44 h | 2.72(56)E-15 |
| Au197(n,g)Au198 | yes | 100.0 | 2.69 d | 1.983(3)E-10 |
| Au197(n,g)Au198 | no | 100.0 | 2.69 d | 2.013(3)E-10 |
| Ti47(n,p)Sc47 | no | 7.30 | 3.43 d | 3.03(12)E-13 |
| Ni58(n,p)Co58 | yes | 68.27 | 72 d | 1.688(14)E-12 |
| Sc45(n,g)Sc46 | yes | 100.0 | 85 d | 5.713(37)E-12 |
| Sc45(n,g)Sc46 | no | 100.0 | 85 d | 6.085(39)E-12 |
| Fe54(n,p)Mg54 | yes | 5.80 | 310 d | 1.53 (19)E-12 |

Figure 4 shows a comparison of the fitted spectrum with the trial spectrum. The fit closely matches the trial spectrum below 3000 keV, but above 3000 keV, the fitted spectrum is higher. This may indicate that the $^{235}U$ cross sections, on which the trial spectrum is based, are too low at high energies.

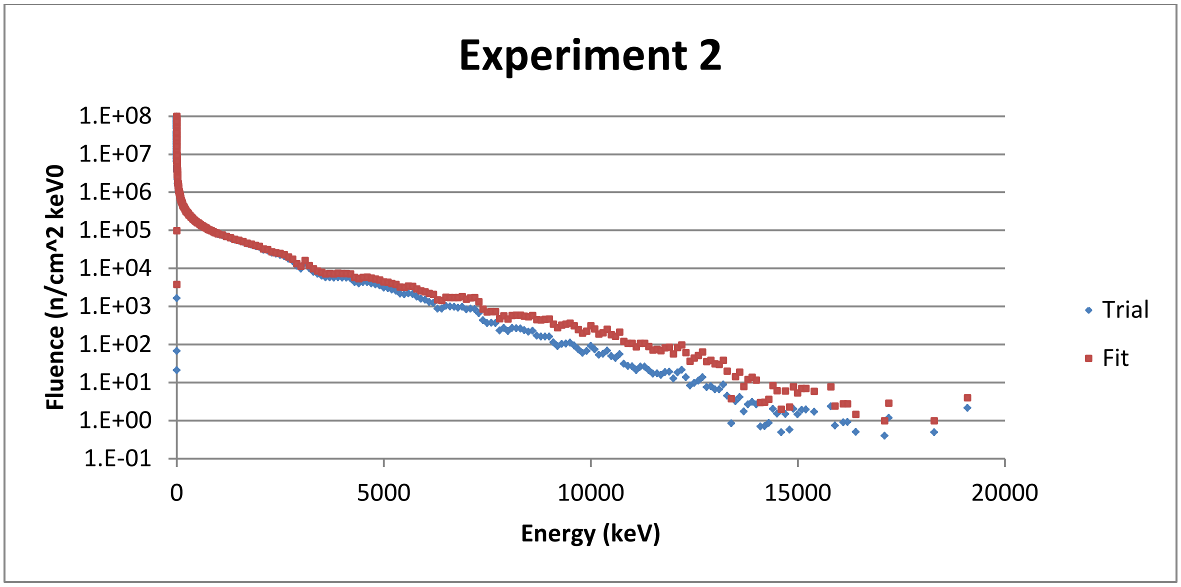


Figure 4. Comparison of the MCNP trial spectrum and the spectrum determined by unfolding the activation foils data for experiment 2, which had 6 graphite plates per unit.

ZEUS Experiment 3

This experiment was similar to experiment 1, but the core loading contained 9 units. Each unit contained one inner HEU disk and one outer HEU ring sandwiched in the middle of four graphite plates. The sample plate was located between units 4 and 5. Table 3 lists the data from the gamma-ray measurements of the activated foils.

Table 3. Experiment 3 Foil Data

| Reaction | Cd Cover? | Isotopic Abundance (%) | Half-life | Ratio |
|---|---|---|---|---|
| Al27(n,p)Mg27 | no | 100.0 | 9.45 min | 5.012(82)E-14 |
| In115(n,g)In116m | yes | 95.70 | 54 m | 6.396(23)E-11 |
| In115(n,g)In116m | no | 95.70 | 54 m | 6.511(26)E-11 |
| Fe56(n,p)Mn56 | yes | 91.72 | 2.57 h | 1.863(54)E-14 |
| Cu63(n,g)Cu64 | no | 69.17 | 12.8 h | 1.116(3)E-11 |
| Cu63(n,g)Cu64 | yes | 69.17 | 12.8 h | 1.011(2)E-11 |
| Mg24(n,p)Na24 | no | 78.99 | 15.06 h | 2.74(20)E-14 |
| Al27(n,a)Na24 | no | 100.00 | 15.06 h | 1.098(33)E-14 |
| Ti48(n,p)Sc48 | no | 73.80 | 44 h | 4.24(55)E-15 |
| Au197(n,g)Au198 | yes | 100.0 | 2.69 d | 1.247(3)E-10 |
| Au197(n,g)Au198 | no | 100.0 | 2.69 d | 1.226(3)E-10 |
| Ti47(n,p)Sc47 | no | 7.30 | 3.43 d | 4.17(12)E-13 |
| Ni58(n,p)Co58 | yes | 68.27 | 72 d | 2.382(15)E-12 |
| Sc45(n,g)Sc46 | no | 100.0 | 85 d | 5.128(33)E-12 |
| Sc45(n,g)Sc46 | yes | 100.0 | 85 d | 5.049(32)E-12 |
| Fe54(n,p)Mg54 | yes | 5.80 | 310 d | 2.03(26)E-12 |

Figure 5 shows a comparison of the fitted spectrum with the trial spectrum. The fit closely matches the trial spectrum below 8000 keV, but above 8000 keV, the fitted spectrum is higher. This may indicate that the $^{235}U$ cross sections, on which the trial spectrum is based, are too low at high energies.

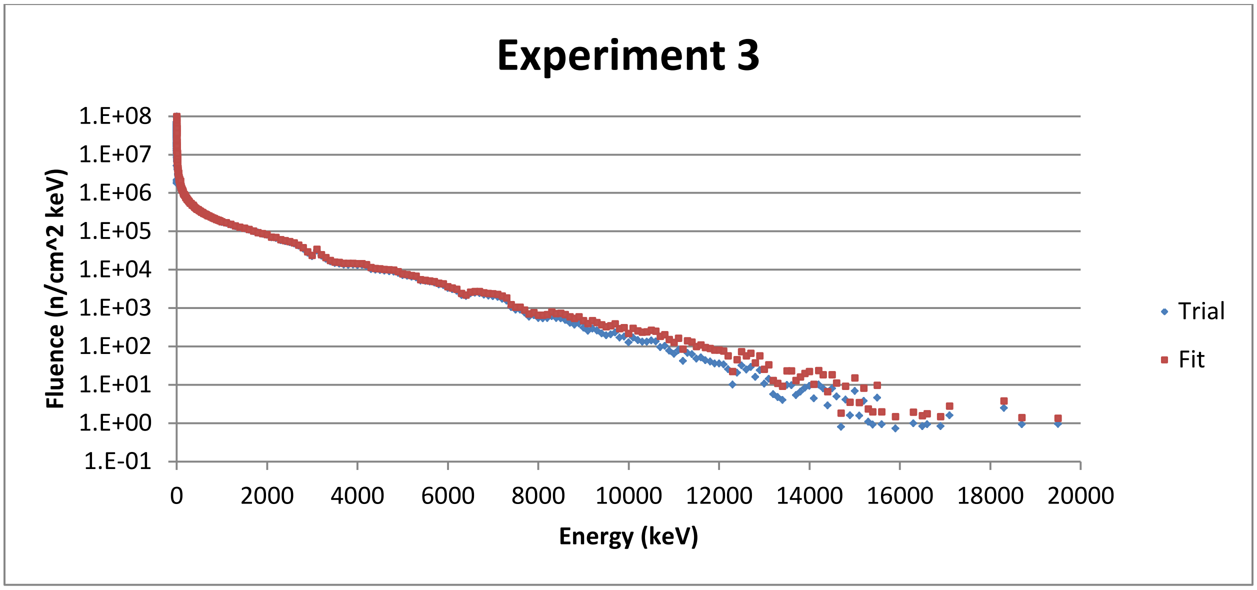


Figure 5. Comparison of the MCNP trial spectrum and the spectrum determined by unfolding the activation foils data for experiment 3, which had 4 graphite plates per unit.

ZEUS Experiment 4

This experiment was similar to experiment 1, but the core loading contained 9 units. Each unit contained one inner HEU disk and one outer HEU ring sandwiched between two graphite plates. The sample plate was located between units 3 and 4. Table 4 lists the data from the gamma-ray measurements of the activated foils.

Table 4. Experiment 4 Foil Data

| Reaction | Cd Cover? | Isotopic Abundance (%) | Half-life | Ratio |
|---|---|---|---|---|
| Al27(n,p)Mg27 | no | 100.0 | 9.45 min | 7.19(10)E-14 |
| In115(n,g)In116m | yes | 95.70 | 54 m | 4.458(19)E-11 |
| In115(n,g)In116m | no | 95.70 | 54 m | 4.575(16)E-11 |
| Fe56(n,p)Mn56 | yes | 91.72 | 2.57 h | 2.903(66)E-14 |
| Cu63(n,g)Cu64 | no | 69.17 | 12.8 h | 6.709(20)E-12 |
| Cu63(n,g)Cu64 | yes | 69.17 | 12.8 h | 6.773(20)E-12 |
| Mg24(n,p)Na24 | no | 78.99 | 15.06 h | 4.40(24)E-14 |
| Al27(n,a)Na24 | no | 100.00 | 15.06 h | 1.858(42)E-14 |
| Ti48(n,p)Sc48 | no | 73.80 | 44 h | 7.00(61)E-15 |
| Au197(n,g)Au198 | yes | 100.0 | 2.69 d | 6.385(19)E-11 |
| Au197(n,g)Au198 | no | 100.0 | 2.69 d | 6.311(19)E-11 |
| Ti47(n,p)Sc47 | no | 7.30 | 3.43 d | 6.16(12)E-13 |
| Ni58(n,p)Co58 | yes | 68.27 | 72 d | 3.415(35)E-12 |
| Sc45(n,g)Sc46 | no | 100.0 | 85 d | 4.120(32)E-12 |
| Sc45(n,g)Sc46 | yes | 100.0 | 85 d | 4.346(19)E-12 |
| Fe54(n,p)Mg54 | yes | 5.80 | 310 d | 2.98(37)E-12 |

Figure 6 shows a comparison of the fitted spectrum with the trial spectrum. The fit closely matches the trial spectrum below 4200 keV and above 13000 keV, but the fit is a little lower between these energies. The agreement is unexpectedly good agreement, especially at high energies. This might be due to uncertainty about the exact configuration when the sample plate was included.

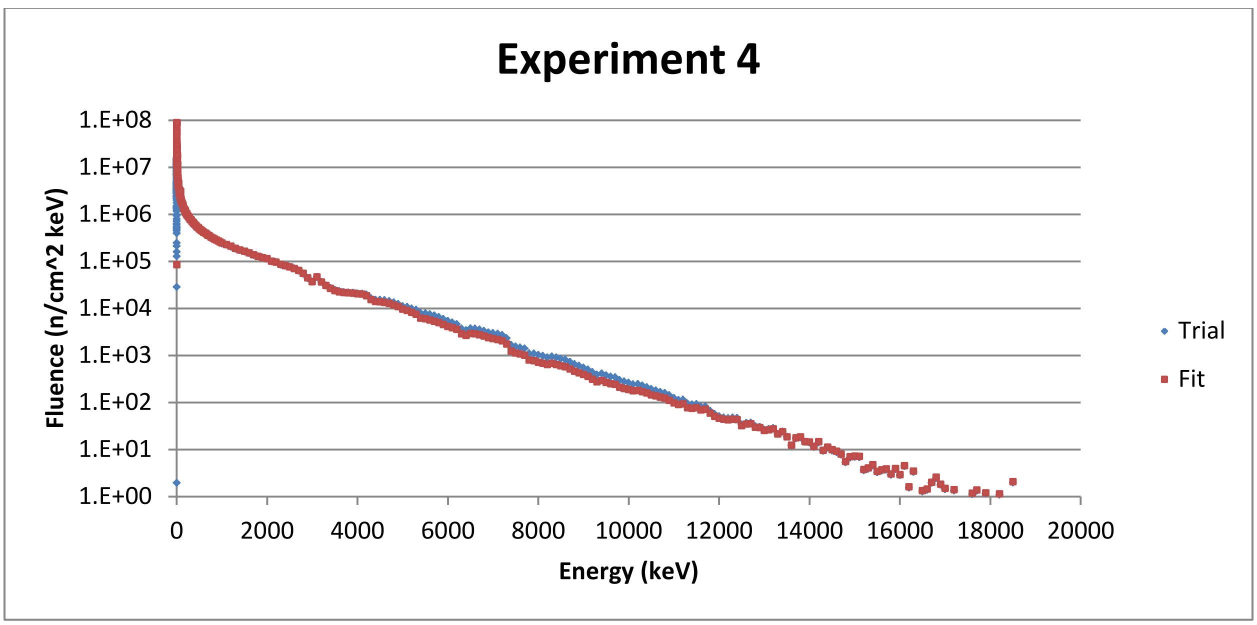


Figure 6. Comparison of the MCNP trial spectrum and the spectrum determined by unfolding the activation foils data for experiment 4, which had 2 graphite plates per unit.

ZEUS Experiment 5

This experiment was similar to experiment 1, but no graphite moderator plates were used. The core loading contained eight inner HEU disk and eight outer HEU rings. The sample plate was located between units 5 and 6. Table 5 lists the data from the gamma-ray measurements of the activated foils.

Table 5. Experiment 5 Foil Data

| **Reaction** | **Cd Cover?** | **Isotopic Abundance (%)** | **Half-life** | **Ratio** |
|---|---|---|---|---|
| Al27(n,p)Mg27 | no | 100.0 | 9.45 min | 1.318(9)E-13 |
| In115(n,g)In116m | yes | 95.70 | 54 m | 3.317(16)E-11 |
| In115(n,g)In116m | no | 95.70 | 54 m | 3.366(18)E-11 |
| Fe56(n,p)Mn56 | yes | 91.72 | 2.57 h | 6.039(88)E-14 |
| Cu63(n,g)Cu64 | no | 69.17 | 12.8 h | 3.341(14)E-12 |
| Cu63(n,g)Cu64 | yes | 69.17 | 12.8 h | 2.922(13)E-12 |
| Mg24(n,p)Na24 | no | 78.99 | 15.06 h | 9.37(31)E-14 |
| Al27(n,a)Na24 | no | 100.00 | 15.06 h | 4.124(60)E-14 |
| Ti48(n,p)Sc48 | no | 73.80 | 44 h | 1.794(60)E-14 |
| Au197(n,g)Au198 | yes | 100.0 | 2.69 d | 2.746(13)E-11 |
| Au197(n,g)Au198 | no | 100.0 | 2.69 d | 2.793(14)E-11 |
| Ti47(n,p)Sc47 | no | 7.30 | 3.43 d | 1.142(14)E-12 |
| Ni58(n,p)Co58 | yes | 68.27 | 72 d | 6.598(25)E-12 |
| Sc45(n,g)Sc46 | no | 100.0 | 85 d | 2.236(13)E-12 |
| Sc45(n,g)Sc46 | yes | 100.0 | 85 d | 2.227(16)E-12 |
| Fe54(n,p)Mg54 | yes | 5.80 | 310 d | 5.11(21)E-12 |

Figure 7 shows a comparison of the fitted spectrum with the trial spectrum. The fit is higher than the trial spectrum at < 2600 keV and at > 7500 keV and lower between these energies. This may indicate that the $^{235}$U cross sections, on which the trial spectrum is based, are too low at high energies.

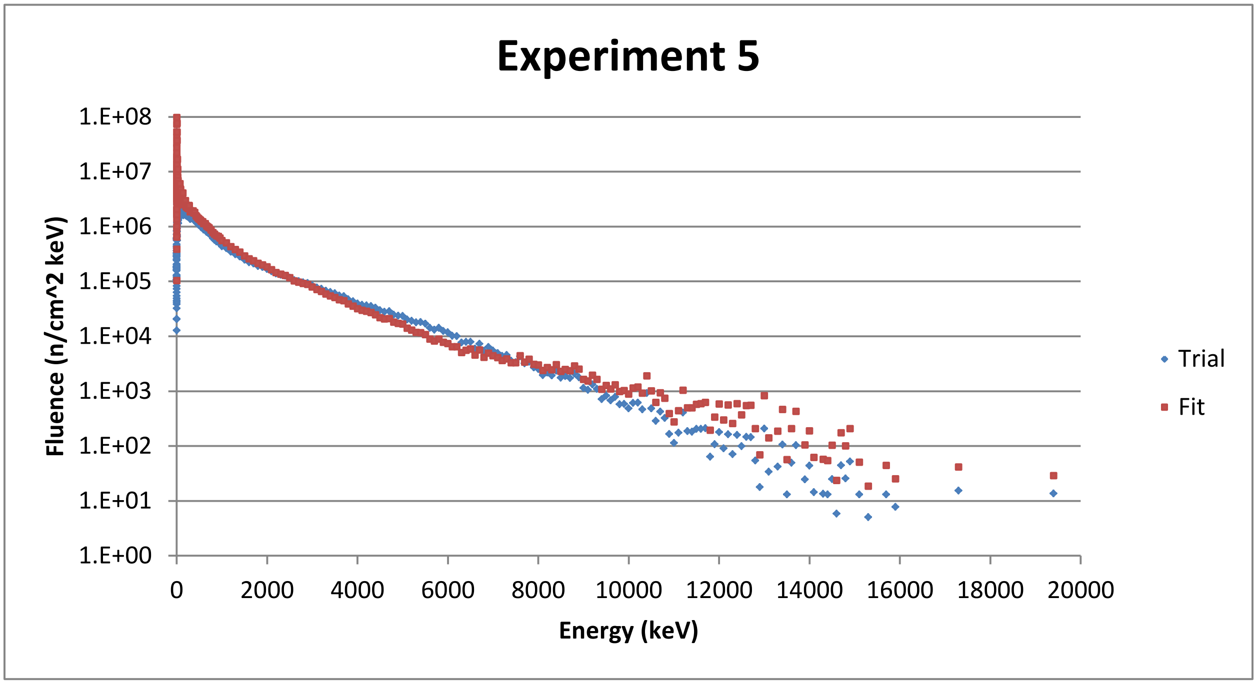


Figure 7. Comparison of the MCNP trial spectrum and the spectrum determined by unfolding the activation foils data for experiment 5, which had no graphite plates.

Figure 8 shows a comparison of the fitted spectra. As expected, the fluence is highest when no graphite was present but decreases as more graphite was included. The shape and separation between the spectra may depend on the location of the sample plate in the loading. The sample plate was in the middle of the loading only in experiment 5. The statistics are poor at > 8000 keV, but these could be improved by much longer MCNP runs (days) or use of the HPC (High Performance Computer) for the trial spectra and the binning of the cross sections for the response functions.

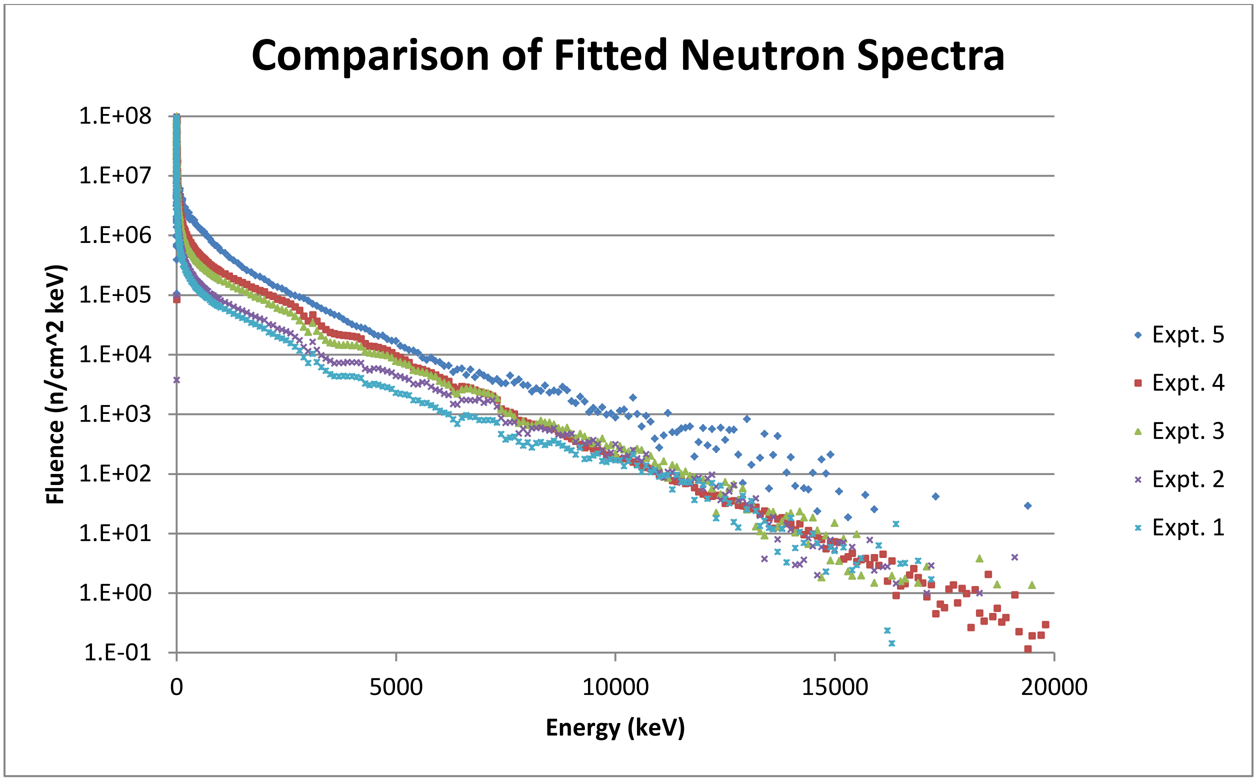


Figure 8. Comparison of the fitted spectra for the five ZEUS experiments.

Figure 9 is an expanded plot of the energy region 0 to 10000 keV. The spectra for the configurations with carbon show some structure caused by reactions on carbon as labeled with a few reactions in the figure whereas the spectrum without carbon (experiment 5) is smooth.

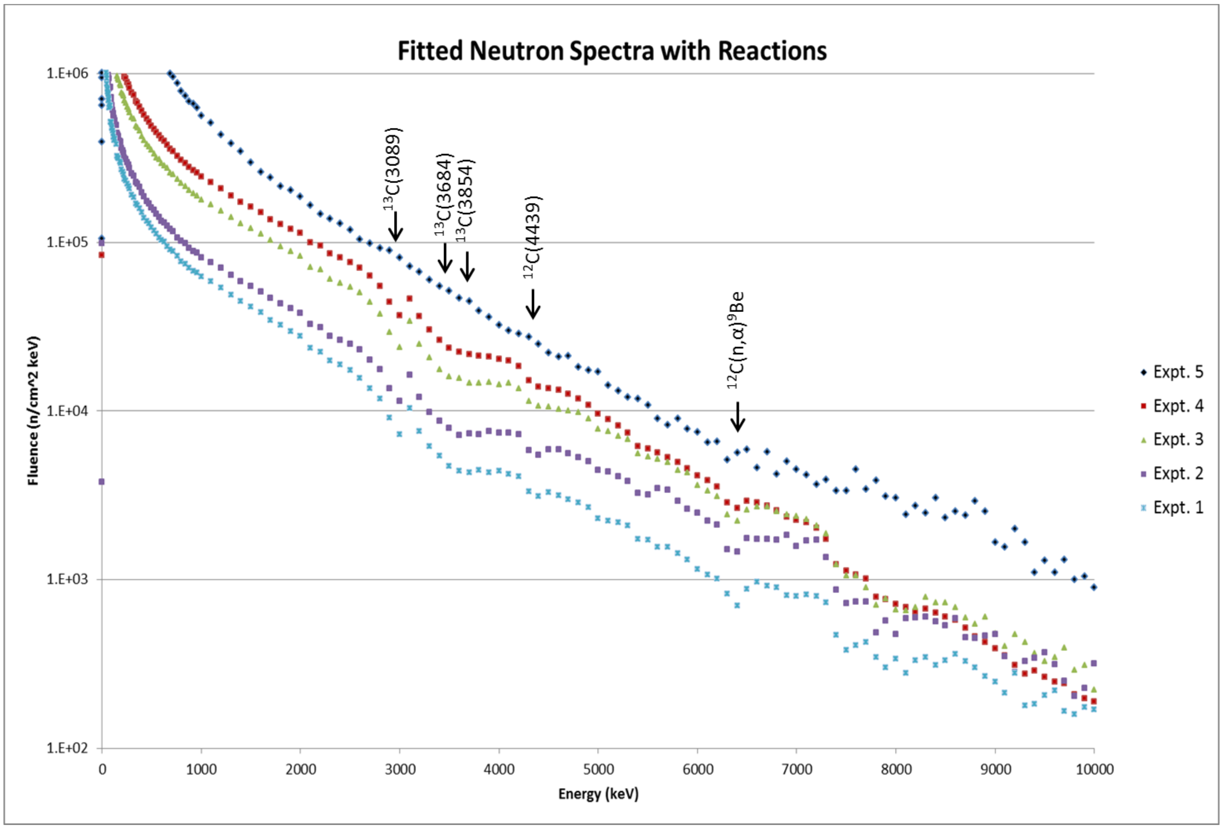


Figure 9. Fitted spectra showing locations of some structures caused by reactions on carbon.

## Conclusions

The Maximum Entropy (MAXED) code has been used to unfold the ZEUS activation foil data taken in 2000 and 2001 to determine the internal neutron spectrum in the five configurations. The unfolded neutron spectrum is higher than the spectrum calculated with MCNP above 6500 keV in four of the five experiments. This suggests that the $^{235}U$ cross sections are too low in this region. The statistics are poor above 10000 keV because the cross sections are small. The statistics could be improved with longer MCNP runs for the response functions binning and the calculations of the neutron spectra. This would require days on a PC, and obviously, a HPC would be much faster. Analysis of this data and other data with different unfolding codes is needed to better understand the unfolding. Also, if the primary interest is in the MeV region, more foils with threshold energies in this region should be included.

# Appendix

## Partial Examples of MAXED files

The MAXED manual obtained with the code from RSICC provides a detailed description of the requirements for these files. The files are in strict FORTRAN formats.

1. Control file

```
0  * Zeus 010 config   number of activated nuclei per target nuclei
   16     0
Al27np              1.318E-13      9.379E-16    0.71     2.0     1
In115ngC            3.317E-11      1.560E-13    0.47     2.0     2
In115ng             3.366E-11      1.778E-13    0.53     2.0     3
Fe56npC             6.039E-14      8.835E-16    1.46     2.0     4
Cu63ng              3.341E-12      1.407E-14    0.42     2.0     5
Cu63ngC             2.922E-12      1.282E-14    0.44     2.0     6
Mg24np              9.367E-14      3.086E-15    3.29     2.0     7
Al27na              4.124E-14      6.048E-16    1.47     2.0     8
Ti48np              1.794E-14      6.031E-16    3.36     2.0     9
Au197ngC            2.746E-11      1.334E-13    0.49     2.0    10
Au197ng             2.793E-11      1.353E-13    0.48     2.0    11
Ti47np              1.142E-12      1.414E-14    1.24     2.0    12
Ni58npC             6.598E-12      2.486E-14    0.38     2.0    13
Sc45ng              2.236E-12      1.313E-14    0.59     2.0    14
Sc45ngC             2.227E-12      1.571E-14    0.71     2.0    15
Fe54npC             5.111E-12      2.064E-13    4.04     2.0    16

Foil             Measurement    Mea stat   % stat   % syst
                                    uncer      uncer    uncer   flag
```

2. Measured data

```
0  * Zeus 010 config   number of activated nuclei per target nuclei
   16     0
Al27np              1.318E-13      9.379E-16    0.71     2.0     1
In115ngC            3.317E-11      1.560E-13    0.47     2.0     2
In115ng             3.366E-11      1.778E-13    0.53     2.0     3
Fe56npC             6.039E-14      8.835E-16    1.46     2.0     4
Cu63ng              3.341E-12      1.407E-14    0.42     2.0     5
Cu63ngC             2.922E-12      1.282E-14    0.44     2.0     6
Mg24np              9.367E-14      3.086E-15    3.29     2.0     7
Al27na              4.124E-14      6.048E-16    1.47     2.0     8
Ti48np              1.794E-14      6.031E-16    3.36     2.0     9
Au197ngC            2.746E-11      1.334E-13    0.49     2.0    10
Au197ng             2.793E-11      1.353E-13    0.48     2.0    11
Ti47np              1.142E-12      1.414E-14    1.24     2.0    12
Ni58npC             6.598E-12      2.486E-14    0.38     2.0    13
Sc45ng              2.236E-12      1.313E-14    0.59     2.0    14
Sc45ngC             2.227E-12      1.571E-14    0.71     2.0    15
Fe54npC             5.111E-12      2.064E-13    4.04     2.0    16

Foil             Measurement    Mea stat   % stat   % syst
                                    uncer      uncer    uncer   flag
```

## 3. Response Functions

```
May 4, 2016  Based on cross sectons calculated with MCNP6
Neutron Response Functions for Zeus
       641    0
1.000E-04       1.050E-04       1.100E-04       1.150E-04       1.200E-04       1.275E-04       1.350E-04       1.425E-04
1.500E-04       1.600E-04       1.700E-04       1.800E-04       1.900E-04       2.000E-04       2.100E-04       2.200E-04
2.300E-04       2.400E-04       2.550E-04       2.700E-04       2.800E-04       3.000E-04       3.200E-04       3.400E-04
3.600E-04       3.800E-04       4.000E-04       4.250E-04       4.500E-04       4.750E-04       5.000E-04       5.250E-04
5.500E-04       5.750E-04       6.000E-04       6.300E-04       6.600E-04       6.900E-04       7.200E-04       7.600E-04
8.000E-04       8.400E-04       8.800E-04       9.200E-04       9.600E-04       1.000E-03       1.050E-03       1.100E-03
1.150E-03       1.200E-03       1.275E-03       1.350E-03       1.425E-03       1.500E-03       1.600E-03       1.700E-03
1.800E-03       1.900E-03       2.000E-03       2.100E-03       2.200E-03       2.300E-03       2.400E-03       2.550E-03
2.700E-03       2.800E-03       3.000E-03       3.200E-03       3.400E-03       3.600E-03       3.800E-03       4.000E-03
4.250E-03       4.500E-03       4.750E-03       5.000E-03       5.250E-03       5.500E-03       5.750E-03       6.000E-03
6.300E-03       6.600E-03       6.900E-03       7.200E-03       7.600E-03       8.000E-03       8.400E-03       8.800E-03
9.200E-03       9.600E-03       1.000E-02       1.050E-02       1.100E-02       1.150E-02       1.200E-02       1.275E-02
1.350E-02       1.425E-02       1.500E-02       1.600E-02       1.700E-02       1.800E-02       1.900E-02       2.000E-02
2.100E-02       2.200E-02       2.300E-02       2.400E-02       2.550E-02       2.700E-02       2.800E-02       3.000E-02
3.200E-02       3.400E-02       3.600E-02       3.800E-02       4.000E-02       4.250E-02       4.500E-02       4.750E-02
5.000E-02       5.250E-02       5.500E-02       5.750E-02       6.000E-02       6.300E-02       6.600E-02       6.900E-02
7.200E-02       7.600E-02       8.000E-02       8.400E-02       8.800E-02       9.200E-02       9.600E-02       1.000E-01
1.050E-01       1.100E-01       1.150E-01       1.200E-01       1.275E-01       1.350E-01       1.425E-01       1.500E-01
1.600E-01       1.700E-01       1.800E-01       1.900E-01       2.000E-01       2.100E-01       2.200E-01       2.300E-01
2.400E-01       2.550E-01       2.700E-01       2.800E-01       3.000E-01       3.200E-01       3.400E-01       3.600E-01
3.800E-01       4.000E-01       4.250E-01       4.500E-01       4.750E-01       5.000E-01       5.250E-01       5.500E-01
5.750E-01       6.000E-01       6.300E-01       6.600E-01       6.900E-01       7.200E-01       7.600E-01       8.000E-01
8.400E-01       8.800E-01       9.200E-01       9.600E-01       1.000E+00       1.050E+00       1.100E+00       1.150E+00
1.200E+00       1.275E+00       1.350E+00       1.425E+00       1.500E+00       1.600E+00       1.700E+00       1.800E+00
1.900E+00       2.000E+00       2.100E+00       2.200E+00       2.300E+00       2.400E+00       2.550E+00       2.700E+00
2.800E+00       3.000E+00       3.200E+00       3.400E+00       3.600E+00       3.800E+00       4.000E+00       4.250E+00
4.500E+00       4.750E+00       5.000E+00       5.250E+00       5.500E+00       5.750E+00       6.000E+00       6.300E+00
6.600E+00       6.900E+00       7.200E+00       7.600E+00       8.000E+00       8.400E+00       8.800E+00       9.200E+00
9.600E+00       1.000E+01       1.050E+01       1.100E+01       1.150E+01       1.200E+01       1.275E+01       1.350E+01
1.425E+01       1.500E+01       1.600E+01       1.700E+01       1.800E+01       1.900E+01       2.000E+01       2.100E+01
2.200E+01       2.300E+01       2.400E+01       2.550E+01       2.700E+01       2.800E+01       3.000E+01       3.200E+01
3.400E+01       3.600E+01       3.800E+01       4.000E+01       4.250E+01       4.500E+01       4.750E+01       5.000E+01
5.250E+01       5.500E+01       5.750E+01       6.000E+01       6.300E+01       6.600E+01       6.900E+01       7.200E+01
```

…

```
         0
        29
In115ng
 1.000E+00      cm^2          0          0    3    1    1    0
3.063E-21       3.006E-21       2.936E-21       2.867E-21       2.801E-21       2.716E-21       2.660E-21       2.571E-21
2.494E-21       2.418E-21       2.357E-21       2.288E-21       2.235E-21       2.169E-21       2.115E-21       2.063E-21
2.023E-21       1.981E-21       1.919E-21       1.875E-21       1.831E-21       1.760E-21       1.706E-21       1.659E-21
1.616E-21       1.568E-21       1.531E-21       1.485E-21       1.448E-21       1.411E-21       1.378E-21       1.342E-21
1.317E-21       1.285E-21       1.262E-21       1.222E-21       1.201E-21       1.169E-21       1.143E-21       1.113E-21
1.085E-21       1.062E-21       1.033E-21       1.018E-21       9.940E-22       9.728E-22       9.464E-22       9.279E-22
9.077E-22       8.842E-22       8.596E-22       8.324E-22       8.125E-22       7.931E-22       7.692E-22       7.459E-22
7.270E-22       7.017E-22       6.904E-22       6.729E-22       6.575E-22       6.436E-22       6.281E-22       6.117E-22
5.944E-22       5.791E-22       5.613E-22       5.442E-22       5.277E-22       5.138E-22       5.013E-22       4.884E-22
4.730E-22       4.582E-22       4.488E-22       4.357E-22       4.270E-22       4.175E-22       4.093E-22       3.998E-22
3.910E-22       3.817E-22       3.743E-22       3.645E-22       3.564E-22       3.482E-22       3.393E-22       3.307E-22
3.252E-22       3.179E-22       3.112E-22       3.035E-22       2.979E-22       2.913E-22       2.840E-22       2.764E-22
2.686E-22       2.631E-22       2.546E-22       2.461E-22       2.406E-22       2.340E-22       2.284E-22       2.240E-22
2.180E-22       2.132E-22       2.091E-22       2.034E-22       1.994E-22       1.946E-22       1.889E-22       1.842E-22
1.786E-22       1.745E-22       1.705E-22       1.668E-22       1.624E-22       1.582E-22       1.538E-22       1.504E-22
1.481E-22       1.446E-22       1.419E-22       1.384E-22       1.358E-22       1.342E-22       1.319E-22       1.294E-22
1.268E-22       1.236E-22       1.217E-22       1.199E-22       1.174E-22       1.153E-22       1.137E-22       1.123E-22
1.107E-22       1.086E-22       1.073E-22       1.053E-22       1.034E-22       1.017E-22       1.004E-22       9.827E-23
9.688E-23       9.575E-23       9.435E-23       9.330E-23       9.272E-23       9.180E-23       9.138E-23       9.065E-23
9.013E-23       9.005E-23       8.975E-23       9.000E-23       8.963E-23       9.025E-23       9.023E-23       9.150E-23
9.252E-23       9.326E-23       9.534E-23       9.739E-23       9.946E-23       1.026E-22       1.058E-22       1.089E-22
1.126E-22       1.176E-22       1.237E-22       1.303E-22       1.372E-22       1.473E-22       1.613E-22       1.770E-22
1.975E-22       2.221E-22       2.517E-22       2.903E-22       3.446E-22       4.306E-22       5.610E-22       7.614E-22
1.260E-21       2.950E-21       1.193E-20       2.595E-20       7.605E-21       1.482E-21       5.970E-22       3.163E-22
1.940E-22       1.308E-22       9.398E-23       7.073E-23       5.465E-23       4.193E-23       3.177E-23       2.623E-23
2.175E-23       1.878E-23       1.965E-23       3.134E-23       2.090E-22       5.890E-22       4.658E-23       1.275E-23
7.123E-24       4.992E-24       3.865E-24       3.192E-24       2.774E-24       2.491E-24       2.301E-24       2.223E-24
2.458E-24       2.517E-24       2.864E-24       4.155E-24       8.010E-24       3.102E-23       7.781E-22       9.848E-23
1.033E-23       4.001E-24       2.212E-24       1.965E-24       1.340E-23       1.461E-23       8.348E-25       4.662E-25
3.311E-25       2.596E-25       2.150E-25       1.958E-25       1.969E-25       2.327E-25       3.635E-25       1.095E-24
8.646E-23       4.625E-24       3.990E-25       1.566E-25       1.094E-25       1.589E-25       9.393E-26       1.059E-25
1.733E-25       5.087E-25       9.642E-23       3.078E-24       2.350E-25       4.719E-24       8.980E-24       8.318E-26
4.488E-26       3.881E-26       5.837E-26       4.071E-24       3.715E-24       2.271E-25       2.973E-24       2.304E-25
2.320E-25       4.592E-23       7.648E-25       1.285E-25       1.482E-23       1.177E-25       2.760E-25       2.781E-26
6.237E-25       6.652E-26       7.421E-24       8.282E-24       1.075E-25       1.579E-24       4.012E-24       1.992E-23
2.984E-24       1.768E-23       7.203E-25       2.125E-23       7.324E-25       1.853E-23       6.668E-26       1.291E-23
2.276E-24       1.497E-25       1.741E-23       4.127E-24       1.139E-24       2.135E-24       5.038E-24       1.961E-24
1.259E-23       2.439E-24       7.537E-24       1.239E-24       4.919E-24       2.588E-24       4.712E-24       2.036E-24
```

…

4. Output File

```
 Fluence spectrum from program MXD_FC33
          1          0
          1         638          638   19900000.0              0
   1.04999999E-04   0.00000000       0.00000000
   1.10000001E-04   0.00000000       0.00000000
   1.15000003E-04   0.00000000       0.00000000
   1.19999997E-04   0.00000000       0.00000000
   1.27499996E-04   0.00000000       0.00000000
   1.34999995E-04   0.00000000       0.00000000
   1.42499994E-04   0.00000000       0.00000000
   1.50000007E-04   0.00000000       0.00000000
   1.59999996E-04   0.00000000       0.00000000
   1.69999999E-04   0.00000000       0.00000000
   1.80000003E-04   0.00000000       0.00000000
   1.90000006E-04   0.00000000       0.00000000
   1.99999995E-04   0.00000000       0.00000000
   2.09999998E-04   0.00000000       0.00000000
   2.20000002E-04   0.00000000       0.00000000
    …
   5000000.00       1680996.25       0.00000000
   5100000.00       1409010.75       0.00000000
   5200000.00       1296849.50       0.00000000
   5300000.00       1189253.50       0.00000000
   5400000.00       1164332.50       0.00000000
   5500000.00       1072786.00       0.00000000
   5600000.00       886573.375       0.00000000
   5700000.00       817353.375       0.00000000
   5800000.00       892325.312       0.00000000
   5900000.00       777368.125       0.00000000
   6000000.00       742762.562       0.00000000
    …
```

5. Default Spectrum

```
        639          0           1           1
  1.00000000             0           0
default spectrum    MAXED RESULT     XXX
 1.0500E-04 1.1000E-04 1.1500E-04 1.2000E-04 1.2750E-04 1.3500E-04 1.4250E-04
 1.5000E-04 1.6000E-04 1.7000E-04 1.8000E-04 1.9000E-04 2.0000E-04 2.1000E-04
 2.2000E-04 2.3000E-04 2.4000E-04 2.5500E-04 2.7000E-04 2.8000E-04 3.0000E-04
 3.2000E-04 3.4000E-04 3.6000E-04 3.8000E-04 4.0000E-04 4.2500E-04 4.5000E-04
 4.7500E-04 5.0000E-04 5.2500E-04 5.5000E-04 5.7500E-04 6.0000E-04 6.3000E-04
 6.6000E-04 6.9000E-04 7.2000E-04 7.6000E-04 8.0000E-04 8.4000E-04 8.8000E-04
 9.2000E-04 9.6000E-04 1.0000E-03 1.0500E-03 1.1000E-03 1.1500E-03 1.2000E-03
 1.2750E-03 1.3500E-03 1.4250E-03 1.5000E-03 1.6000E-03 1.7000E-03 1.8000E-03
 1.9000E-03 2.0000E-03 2.1000E-03 2.2000E-03 2.3000E-03 2.4000E-03 2.5500E-03
 2.7000E-03 2.8000E-03 3.0000E-03 3.2000E-03 3.4000E-03 3.6000E-03 3.8000E-03
 4.0000E-03 4.2500E-03 4.5000E-03 4.7500E-03 5.0000E-03 5.2500E-03 5.5000E-03
 5.7500E-03 6.0000E-03 6.3000E-03 6.6000E-03 6.9000E-03 7.2000E-03 7.6000E-03
 8.0000E-03 8.4000E-03 8.8000E-03 9.2000E-03 9.6000E-03 1.0000E-02 1.0500E-02
 1.1000E-02 1.1500E-02 1.2000E-02 1.2750E-02 1.3500E-02 1.4250E-02 1.5000E-02
 1.6000E-02 1.7000E-02 1.8000E-02 1.9000E-02 2.0000E-02 2.1000E-02 2.2000E-02
 2.3000E-02 2.4000E-02 2.5500E-02 2.7000E-02 2.8000E-02 3.0000E-02 3.2000E-02
 3.4000E-02 3.6000E-02 3.8000E-02 4.0000E-02 4.2500E-02 4.5000E-02 4.7500E-02
 5.0000E-02 5.2500E-02 5.5000E-02 5.7500E-02 6.0000E-02 6.3000E-02 6.6000E-02
 6.9000E-02 7.2000E-02 7.6000E-02 8.0000E-02 8.4000E-02 8.8000E-02 9.2000E-02
 9.6000E-02 1.0000E-01 1.0500E-01 1.1000E-01 1.1500E-01 1.2000E-01 1.2750E-01
 ….
```

| | | | | | | |
|---|---|---|---|---|---|---|
| 1.4552E+06 | 9.9830E+05 | 9.1810E+05 | 1.2346E+06 | 1.5028E+06 | 1.7060E+06 | 1.4832E+06 |
| 1.2303E+06 | 1.9101E+06 | 1.7592E+06 | 1.3727E+06 | 1.9441E+06 | 1.9054E+06 | 3.5951E+06 |
| 3.8255E+06 | 1.6560E+06 | 3.5226E+06 | 4.7418E+06 | 3.7452E+06 | 2.2837E+06 | 2.6374E+06 |
| 3.4004E+06 | 4.6505E+06 | 4.4576E+06 | 5.6846E+06 | 6.7031E+06 | 6.0741E+06 | 4.6176E+06 |
| 3.7366E+06 | 4.7016E+06 | 7.1461E+06 | 6.7433E+06 | 6.6917E+06 | 9.3883E+06 | 8.3954E+06 |
| 1.0116E+07 | 7.7359E+06 | 6.0616E+06 | 6.2989E+06 | 6.7720E+06 | 7.1813E+06 | 1.0016E+07 |
| 9.4600E+06 | 1.0743E+07 | 1.0383E+07 | 1.7400E+07 | 1.9110E+07 | 1.3840E+07 | 1.2042E+07 |
| 1.6682E+07 | 1.7447E+07 | 1.8728E+07 | 1.9930E+07 | 1.6751E+07 | 1.5832E+07 | 1.6817E+07 |
| 1.5358E+07 | 1.5835E+07 | 2.2675E+07 | 2.6101E+07 | 1.7310E+07 | 2.7272E+07 | 2.8484E+07 |
| 2.8076E+07 | 2.8908E+07 | 2.6529E+07 | 2.7293E+07 | 3.0173E+07 | 2.8569E+07 | 2.7395E+07 |
| 2.6344E+07 | 2.5424E+07 | 2.3962E+07 | 2.3848E+07 | 2.2096E+07 | 2.6660E+07 | 2.4067E+07 |
| 2.3308E+07 | 2.2278E+07 | 2.7279E+07 | 2.4517E+07 | 2.2901E+07 | 2.1277E+07 | 2.0684E+07 |
| 1.9563E+07 | 1.7595E+07 | 4.0172E+07 | 3.4982E+07 | 3.1279E+07 | 2.8596E+07 | 2.5021E+07 |
| 2.2477E+07 | 2.1162E+07 | 1.9080E+07 | 1.8241E+07 | 1.6893E+07 | 1.5313E+07 | 1.3899E+07 |

…

## References


[1] R. D. Mosteller, R. W. Brewer, and J. Sapir, "The Initial Set of ZEUS Experiments: Intermediate-spectrum Critical Assemblies with a Graphite-HEU Core Surrounded by a Copper Reflector," NEA/NSC/DOC/(9s5)03/II, Volume II, HEU-MET-INTER-006, Revision 4, September 30, 2004.

[2] R. D. Mosteller, "The Unmoderated ZEUS Experiment: A Cylindrical HEU Core Surrounded by a Copper Reflector," NEA/NSC/DOC/(95)03/II, Volume II, HEU-MET-FAST-073, September 30, 2005.

[3] J. A. Grundl, "Study of Fission Neutron Spectra with High-energy Activation Detectors," Los Alamos National Laboratory report LAMS-2883 (1963).

[4] W. N. McElroy, S. Berg, T. Crockett, an R. Hawkins, "A Computer-Automated Iterative Method for Neutron Flux Spectral Determination by Foil Activation," AFWL-TR-67-41, Vol. 1, Air Force Weapons Laboratory, Kirkland, New Mexico, July 1967.

[5] P. J. Griffin, J. G. Kelly, and J. W. VanDenburg, "User's Manual for SNL-SAND-II Code," Sandia Report SAND93-3957, April 1994.

[6] Z. A. Kulage, C. H. Castano, S. Usman, and G. Mueller, "Characterization of the neutron flux energy spectrum at the Missouri University of Science and Technology Research Reactor (MSTR)," Nucl. Eng. Des. **261** 174-180 (2013).

[7] M. R. Halstead, S. Lee, J. Petroskyl, A. Bickley, and P. Sokol, "Neutron Energy Spectrum Characterization on TMR-1 at the Indiana University Neutron Source," Physics Procedia **26** 188-195 (2012).

[8] https://www.oecd-nea.org/tools/abstract/detail/nea-1665.

[9] F. Z. Dehimi, A. Seghour, and S. E. H. Abaidia, "Unfolding of Neutron Energy Spectra with Fisher Regularisation," IEEE Trans. Nucl. Sci. **57** 768-774 (2010).

[10] V. Suman, S.P. Tripathy, C. Sunil, A. A. Shanbhag, S. Paul, G. S. Sahoo, T. Bandyopadhyay, and P. K. Sarkar, "Measurement of Neutron Energy Distributions from p+Be Reaction at 20 MeV Using Threshold Activation Foils," IEEE Trans. Nucl. Sci. **63** 2283-2292 (2016).

[11] A. Seghour and F. Z. Seghour, "Neutron energy spectra unfolding from foil activation detector measurements with MINUIT," Nucl. Instr. Meth. A **555** 347-355 (2005).

[12] S. P. Tripathy, C. Sunil, M. Nandy, P. K. Nandy, P. K. Sarkar, D. N. Sharma, and B. Mukherjee, "Activation foils unfolding for neutron spectrometry: Comparison of different deconvolution methods," Nucl. Instr. Meth. A **583** 421-425 (2007).

[13] M. Reginatto and P. Goldhagen, "MAXED, a Computer Code for the Deconvolution of Multisphere Neutron Spectrometer Data Using the Maximum Entropy Method," Department of Energy, Environmental Measurements Laboratory report EML-595 (1998).

[14] Rooney, B., Garner, S., Felsher, P., Karpius, P., (2015), PeakEasy 4.84 (Computer Program), Los Alamos National Laboratory, Release LA-CC-13-040, https://PeakEasy.lanl.gov.

[15] LANL drawing 128Y-271100 (2/12/02).